

# CONCEPTUAL LAYOUT OF A NEW SHORT-PULSE RADIATION SOURCE AT DELTA BASED ON ECHO-ENABLED HARMONIC GENERATION

R. Molo\*, M. Bakr, M. Höner, H. Huck, S. Khan, A. Nowaczyk,  
A. Schick, P. Ungelenk, M. Zeinalzadeh,

Zentrum für Synchrotronstrahlung, TU Dortmund University, 44221 Dortmund, Germany

## Abstract

As an upgrade of the present coherent harmonic generation (CHG) source at the DELTA storage ring, the installation of an additional undulator to implement and study the echo-enabled harmonic generation (EEHG) scheme is planned. Compared to the CHG scheme, EEHG allows to produce radiation of shorter wavelengths. In order to avoid dispersive distortions, all undulators should be placed along a straight line. This requires to increase the length of the present straight section by rearranging several magnets and vacuum components as well as a significant modification of the storage-ring optics.

## INTRODUCTION

DELTA is a synchrotron light source with a circumference of 115.2 m, operated by the TU Dortmund University. Its nominal electron beam energy is 1.5 GeV. The storage ring shown in Fig. 1 comprises two undulators (U55, U250) and a superconducting wiggler (SAW).

The pulse duration of short-wavelength synchrotron radiation is given by the bunch length and is typically 100 ps (FWHM). On the other hand, commercial femtosecond lasers have pulse durations of about 20-40 fs, but their wavelengths are in the near-visible regime.

Several ways have been proposed to produce radiation with short wavelengths (< 200 nm) as well as short pulse duration ( $\leq 100$  fs). One of them is the coherent harmonic generation (CHG) technique [1, 2, 3] which has been

shifts at DELTA [4]. This paper will discuss echo-enabled harmonic generation (EEHG) [5] as a possible upgrade of CHG in order to obtain shorter wavelengths. EEHG was experimentally tested for the first time at SLAC [6], and studies exist to apply it at storage rings as well [7].

## THEORY

CHG requires a femtosecond laser system, two undulators and a chicane as shown schematically in Fig. 2. A short laser pulse propagates through the first undulator (modulator) and interacts with co-propagating electrons. This interaction modulates the electron energy sinusoidally with the periodicity of the laser wavelength. Since the laser pulse is typically 1000 times shorter than the electron distribution, only a small slice of the bunch is modulated. Inside the following chicane, the path lengths of the electrons depend on their energy, converting the energy modulation into a density modulation (known as microbunching). The desired longitudinal dispersion can be estimated to be

$$R_{56} \approx \frac{\lambda}{4} \frac{E}{\Delta E},$$

where  $\Delta E$  is the amplitude of the energy modulation,  $E$  is the nominal electron energy, and  $\lambda$  is the laser wavelength.

In contrast to the rest of the bunch, the microbunches radiate coherently and therefore more intense at the initial laser wavelength and harmonics thereof. The second undulator (radiator) is tuned to the desired harmonic. The

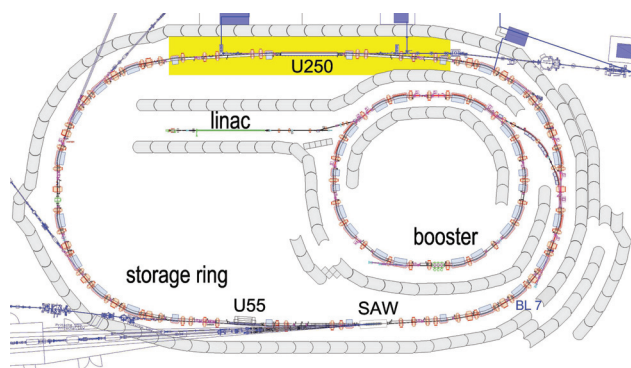


Figure 1: Schematic diagram of the DELTA synchrotron radiation facility. The yellow field denotes the northern part of DELTA where the CHG setup is located.

recently commissioned during machine studies and user

\* robert.molo@tu-dortmund.de

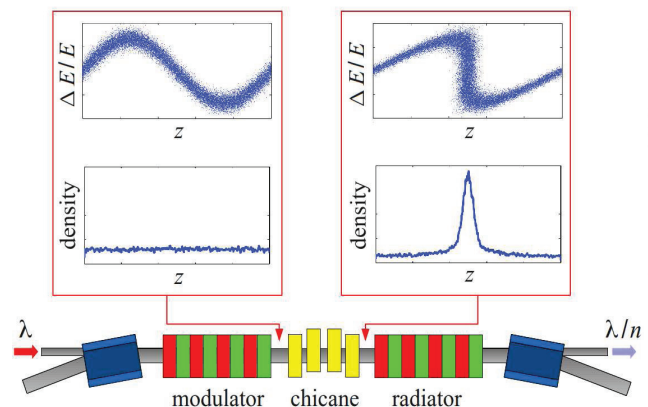


Figure 2: Schematic diagram of the CHG scheme with two undulators and one chicane. The longitudinal phase space diagrams show the electron distribution before and after the chicane.

radiated power from the microbunches at the  $n$ th harmonic of the laser wavelength is given by [8]

$$P_n(\lambda) \sim N^2 b_n^2(\lambda),$$

where  $N$  is the number of modulated electrons in the bunch, and  $b_n(\lambda)$  is the so-called bunching factor that describes the degree of bunching between 0 (no microbunching) and 1 (perfect microbunching). Using a periodic electron bunch model and a plane electromagnetic wave leads to an analytical formula of the bunching factor [8]

$$b_n(\lambda) \sim e^{-n^2}$$

decreasing exponentially with the square of the harmonic number. This limits the ability of CHG to produce harmonics significantly higher than 5. To overcome this limitation, the EEHG technique was proposed [5].

In contrast to CHG, the EEHG scheme requires three undulators and two chicanes (Fig. 3). In this configuration, the electron beam is modulated twice by two laser pulses.

The interaction in the first undulator modulates the electron energy sinusoidally. The first chicane has a large  $R_{56}^1$  ( $\sim 1$  mm) which tilts the electron distribution in the phase space so strongly that almost horizontal stripes are generated. The electrons interact again with a laser pulse in the second undulator. The second chicane with a moderate  $R_{56}^2$  produces a density modulation with a high harmonic content. For EEHG, the optimized bunching factor scales with the harmonic number as [9]

$$b_n(\lambda) \sim n^{-\frac{1}{3}}.$$

This allows to reach higher harmonics of the external laser and shorter wavelengths compared to CHG.

### EEHG AT DELTA

The planar electromagnetic undulator U250 located in the northern part of DELTA consists of 19 periods of

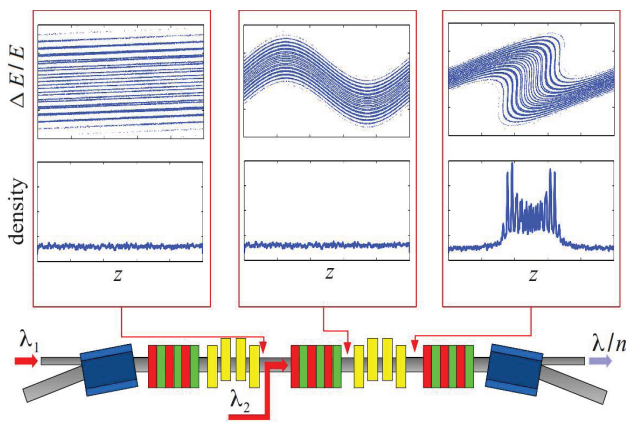


Figure 3: Sketch of the EEHG scheme with three undulators and two chicanes. The longitudinal phase space diagrams show the electron distribution after the first chicane, after the second undulator and after the second chicane.

250 mm each. This undulator is currently employed to produce harmonics using the CHG technique. In the center of the U250, six poles can be driven at higher current to form a chicane.

The undulator is placed in a straight section between two 3- and 7-degree dipoles. Since the free space is limited, additional undulators and chicanes for EEHG cannot be installed here. On the other hand, all undulators should be installed along a straight section to avoid dispersive distortions ( $R_{51}$  and  $R_{52}$ ). The straight section A (see Fig. 4) can be extended by changing the bending angle of the dipoles. The rest of the storage ring will remain unchanged apart from the fact that the circumference will increase.

### New Dipole Configuration

Exchanging the 3- and 7-degree dipoles will increase the length of the straight section A from 6.39 m to about 16 m. The currently used dipoles and quadrupoles can be reused. One benefit of not choosing other possible angles is that the present dipole chambers can be employed. In this configuration, the total storage ring circumference will be increased by about 3 cm, which is tolerable.

### New Quadrupole Configuration

Such a significant modification of the dipole magnet configuration requires a new arrangement of quadrupoles. Figure 4 shows a solution with only one additional quadrupole. Simulations for this new optics at DELTA were performed using the code *elegant* [10], optimizing the quadrupole strengths and positions.

Figure 5 shows a comparison between the present (black line) and the new (red line) horizontal beta function  $\beta_x$  at DELTA. The maximum of the present  $\beta_x$  is about 40 m whereas the  $\beta_x$  of the new lattice does not exceed 20 m. The new and the current beta functions agree well outside the northern section of DELTA. For the new and old lattice, the  $\beta_x$  is highly symmetric around 29 m.

Figure 6 displays the vertical beta function  $\beta_y$  calculated for the present (black line) and new (red line) lattice configuration. In contrast to  $\beta_x$ , a pronounced asymmetry around the U250 is observed for the present lattice caused by the focusing effect of the superconducting wiggler SAW. The maximum of the  $\beta_y$  is presently about 100 m. For the new lattice, the  $\beta_y$  is much smaller in the vicinity of the U250, improving the Coulomb lifetime, and otherwise similar to the present  $\beta_y$ .

In addition to the beta function, the dispersion function influences the beam size as well. Insertion devices are usually installed in sections with low dispersion in order to minimize the beam size of the radiation source. Figure 7 shows the present horizontal dispersion (black line) and the future horizontal dispersion (red line). In the future lattice, the dispersion at the U250 is smaller than presently.

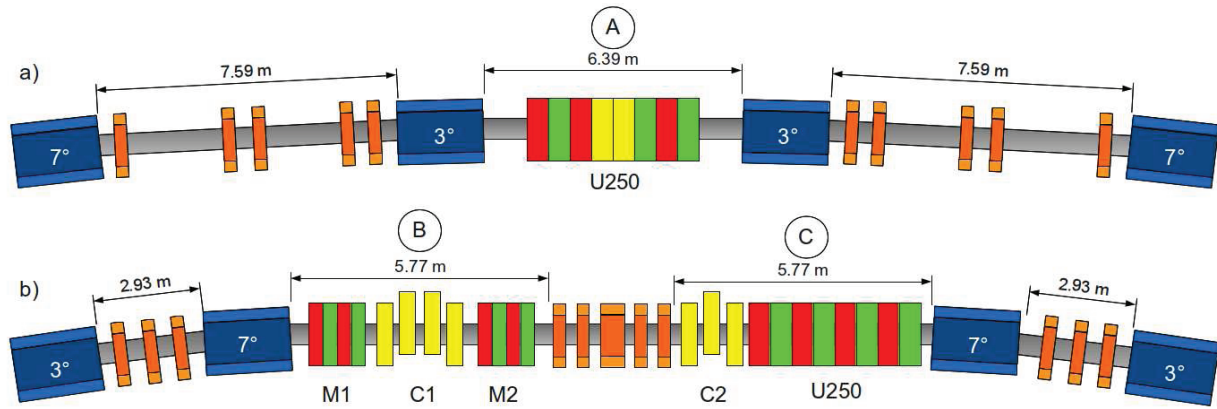


Figure 4: Schematic view of the northern part of DELTA. The orange, blue, and yellow blocks represent quadrupoles, dipoles, and chicane magnets ( $C1$ ,  $C2$ ), respectively. a) The present CHG setup. The undulator U250 is situated in section  $A$  between the 3-degree magnets. b) A possible EEHG setup. Due to the exchange of the 3- and 7-degree dipoles, the straight section is largely extended.

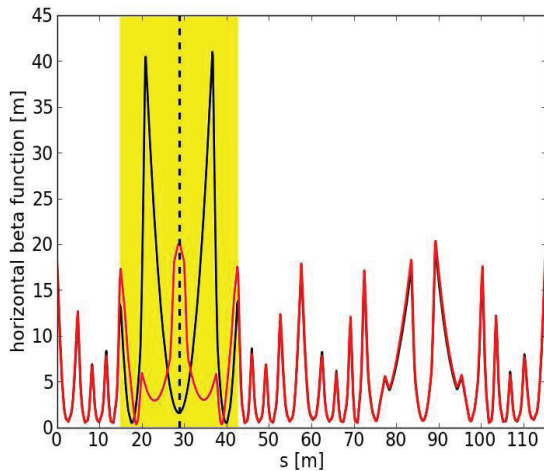


Figure 5: The present (black) and future (red) horizontal beta function versus distance. The yellow colored area denotes the region in which EEHG will be installed. The center of the undulator is located at 29 m (dashed vertical line).

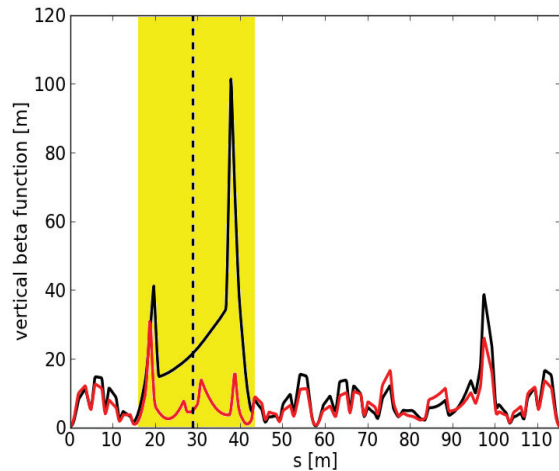


Figure 6: The present (black) and future (red) vertical beta function versus distance. The pronounced asymmetry around the U250 is due to the focusing effect of the SAW.

### New Sextupole Configuration

In the northern part of DELTA to be modified, there are no sextupoles. Simulations revealed that the position of the presently used sextupoles in the other parts of DELTA can be retained. However, their strength has to be changed in order to compensate chromaticity. The simulated dynamic aperture is shown in Fig. 8.

### Insertion Devices

The new arrangement of dipoles and quadrupoles necessary for EEHG is schematically shown in Fig. 4. The two straight sections  $B$  and  $C$  offer enough space for three un-

dulators and two chicanes. Both undulators  $M1$  and  $M2$  will be about 1.5 m long and installed in straight section  $B$ . Between them, a chicane  $C1$  with a  $R_{56}$  in the order of 1 mm will be installed. In section  $C$ , the undulator U250 will be used as radiator. A second chicane  $C2$  with moderate  $R_{56}$  in the range of several microns will be placed preceding the U250 undulator. A comparison between the present and the EEHG lattice properties is given in Tab. 1.

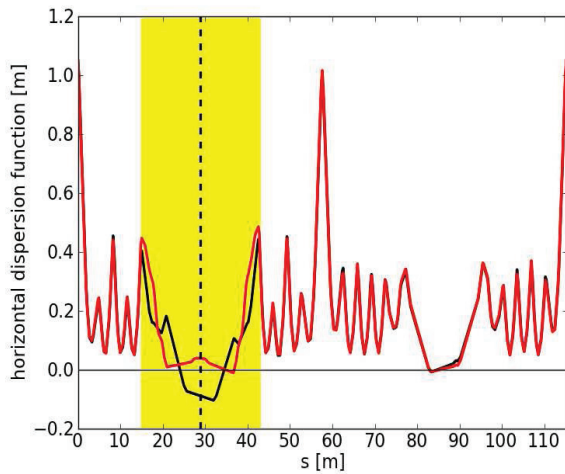


Figure 7: The present (black) and future (red) horizontal dispersion versus distance.

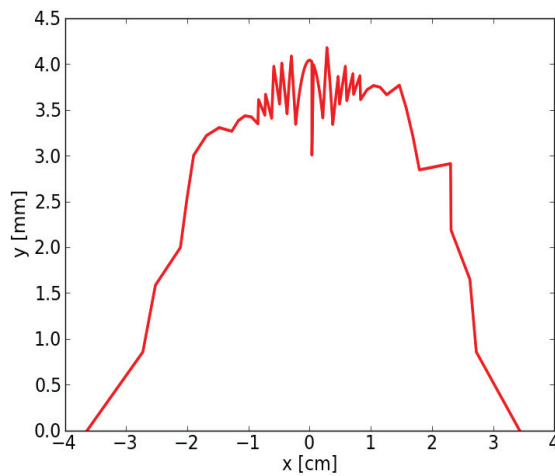


Figure 8: Dynamic aperture estimated by tracking electrons over 10 ms corresponding to the transverse damping time.

Table 1: Lattice Properties

lattice	present	EEHG
circumference	115.20 m	115.23 m
straight sections (north part)	1×6.39 m	2×5.77 m
max. horizontal beta function	41 m	20 m
max. vertical beta function	101 m	31 m
horizontal tune	9.20	9.29
vertical tune	3.37	4.27

## REFERENCES

- [1] B. Girard et al., Phys. Rev. Lett. 53, 2405 (1984).
- [2] G. DeNinno et al., Phys. Rev. Lett. 101, 053902 (2008).
- [3] M. Labat et al., Eur. Phys. J. D 44, 187 (2007).
- [4] H. Huck et al., this conference.
- [5] G. Stupakov, Phys. Rev. Lett. 102, 074801 (2009).
- [6] D. Xiang et al., Phys. Rev. Lett. 105, 114801 (2010).
- [7] C. Evain et al., IPAC'10, 2308 (2010).
- [8] L.H. Yu, Phys. Rev. A 44, 5178 (1991).
- [9] D. Xiang and G. Stupakov, Phys. Rev. ST Accel. Beams 12, 030702 (2009).
- [10] M. Borland, Advanced Photon Source LS-287 (2000).

## CONCLUSIONS

In this work, a possible upgrade scenario of the coherent harmonic generation (CHG) technique has been proposed, and the applicability of echo-enabled harmonic generation (EEHG) at DELTA has been studied. The proposed solution allows to use the present dipoles, quadrupoles and most of the present vacuum chambers. Instead of using two lasers, one can use the present laser system and split the laser pulse. The beta functions of the new lattice are smaller than those of the present lattice, thus an improvement of the aperture-limited beam lifetime can be expected. Pump-probe experiments using EEHG pulses will be performed using the pump-pulse laser beamline which is presently under construction.